HHS Public Access

Author manuscript

Phys Med. Author manuscript; available in PMC 2020 October 01.

Published in final edited form as:

Phys Med. 2020 August ; 76: 142–149. doi:10.1016/j.ejmp.2020.06.026.

Time and Frequency to Observe Fiducial Markers in MLC-Modulated Fields during Prostate IMRT/VMAT Beam Delivery

Qianqian Xu[1], **Xu Tong**[1], **Muhan Lin**[2], **Xiaoming Chen**[2], **Ahmed ElDib**[2], **Teh Lin**[2], **Lili Chen**[2], **C-M Charlie Ma**[2]

[1]Radiation Oncology Department, 3rd Affiliated Hospital of Qiqihar Medical University, Qiqihar, China

[2]Radiation Oncology Department, Fox Chase Cancer Center, Philadelphia, PA

Abstract

Objective—This work investigates the time and frequency to observe fiducial markers in MLC-modulated fields during intensity-modulated radiotherapy (IMRT) and volumetric-modulated arc therapy (VMAT) beam delivery for real-time prostate localization.

Methods—Thirty seven prostate patients treated with IMRT or VMAT were included in this retrospective study. DRR images were generated for all MLC segments/control points using the TPS. The MLC leaf pattern of each control point was overlaid on the DRR, and the number of fiducials within the MLC opening was analyzed. EPID images of fiducials in a pelvic phantom were obtained to demonstrate the fiducial visibility during modulated beam delivery.

Results—Gold fiducials were visible on EPID images. The probability of seeing a number of fiducials within the MLC opening was analyzed. At least one fiducial was visible during 42±2% and 52±2% beam-on time for IMRT of the prostate with and without lymph nodes, and during 85±4% and 88±4% beam-on time for VMAT of the prostate with and without lymph nodes, respectively. The mean time interval to observe at least one fiducial was 8.4±0.7 and 5.9±0.5 seconds for IMRT of the prostate with and without the lymph nodes, respectively, and 1.6±0.1 seconds for VMAT prostate patients. The estimated potential dosimetric uncertainty was 7% and 2% for IMRT and VMAT, respectively.

Conclusions—Our results demonstrated that the time and frequency to observe fiducial markers in MLC-modulated fields during IMRT/VMAT beam delivery were adequate for real-time prostate localization. The beam's eye view fiducial positions could be used for intra-fractional target monitoring and motion correction in prostate radiotherapy.

Keywords

EPID; DRR; fiducial markers; intra-fraction organ motion; real-time target localization; IMRT; VMAT

Corresponding author: C-M Charlie Ma, Charlie.Ma@fccc.edu.
First author: Qianqian Xu

1. Introduction

In the practice of radiotherapy, the accuracy of target localization is very important for improving the local control rate of tumors and sparing nearby critical structures. With the development of radiotherapy and the widespread application of computer technology, advanced conformal radiotherapy has gradually replaced conventional radiotherapy with more precise and sophisticated delivery techniques, such as intensity modulated radiation therapy (IMRT) and volumetric modulated radiation therapy (VMAT). Accurate dose delivery for IMRT and VMAT relies on advances in treatment optimization software, computerized beam delivery hardware and imaging guidance technology for patient setup and target localization prior to and during IMRT and VMAT treatments.

Prostate cancer remains a major source of morbidity and mortality in the United States and worldwide. Significant prostate (target) motion related to bladder and rectal volume change during daily radiation treatments can occur during a course of radiotherapy. New advances in image-guided radiotherapy (IGRT) technology have led to more precise target alignment between treatment fractions and during treatment delivery [1]. The widespread application of IMRT and VMAT with image guidance for prostate radiotherapy has greatly refined the specificity of radiation delivery to target cancerous tissue while minimizing collateral damage to surrounding structures such as the genitourinary system [2,3]. Different techniques have been developed to correct target motion for prostate IMRT/VMAT. Inter-fractional motion from the daily setup variation has been addressed by ultrasound (US), kilovoltage (kV) or megavoltage (MV) x-ray imaging using implanted fiducial markers (FM), and cone beam computed tomography (CBCT) [1,4,5]. Technologies such as real-time orthogonal x-ray imaging, kilovoltage intrafraction monitoring (KIM), implanted radiofrequency markers and cine magnetic resonance imaging [1,6–9] have been used to monitor and correct intrafractional motion of the prostate. For all of these methods, the primary approach is to determine the position of the prostate, adjust the target position by adjustment of the treatment couch or MLC (on conventional clinical accelerators), or the treatment head (on the CyberKnife system), and proceed with targeted radiation delivery. The need to account for positional variation is clinically significant due to the potential dosimetric implications for tumor control and toxicity to surrounding normal tissues [10].

Real-time target localization is more important to hypo-fractionated treatment schemes and stereotactic body radiation therapy (SBRT) because of the increased prescription dose to the target and decreased target margins used in these treatments [11]. It was shown that a small fraction (~4%) of prostate patients may exhibit large prostate motion (> 5mm) in more than 25% of treatment fractions [8]. Recent prostate SBRT trials have recommended the use of real-time monitoring systems such as electromagnetic transponders (Calypso Extracranial Tracking, Varian Medical Systems, Palo Alto, CA) and x-ray/fiducial marker tracking (Accuray Inc., Sunnyvale, CA) [12,13]. The advantages of electromagnetic transponders include the efficiency for patient setup and real-time monitoring of target motion [8,12,14]. However, not all patients can be implanted with such transponders due to medical reasons, and once the transponders are implanted, MR imaging cannot be performed due to the large artifacts induced by the transponders. Since the transponders cannot provide the 3D anatomy information of the target and critical structures, and only the centroid position of the

implanted transponders is generally used for the localization process, the effects of organ deformation cannot be adequately corrected. Furthermore, the effects of rotational changes of the prostate due to rectal and bladder volume change are generally ignored due to either the lack of methods to correct rotational movements and/or the large uncertainties in estimating the rotation angles of the prostate, which can be affected significantly by organ deformation and transponder migration [14]. On the other hand, the CyberKnife system provides real-time tracking of the treatment target using two x-ray panels and implanted radio-opaque fiducials. X-ray imaging together with radio-opaque fiducial markers is an effective way to localize the prostate target by comparing the locations of the fiducial markers on the x-ray images and those on DRR images pre-generated from the planning CT [5–7]. An intrafraction motion review (IMR) system has been available, which allows for automatic fiducial marker detection and automatic beam hold [15]. However, like the Calypso system, x-ray imaging/radiopaque marker-based IGRT systems do not provide the 3D anatomy information and cannot correct the effects of organ deformation. Also, x-ray imaging will result in additional radiation exposure to the patient; typical CyberKnife SBRT treatments last 20–60 minutes and the radiation dose resulting from the continuous x-ray imaging process may become significant [16].

Electronic portal imaging device (EPID) has become widely available in recent years primarily for patient positioning and field verification to reduce irradiation errors [17,18]. As a real-time digital radiation fluence verification system, EPID has been investigated as a dosimetry verification tool for treatment plan QA, dose delivery verification, and online image guidance for target localization [19–24]. EPID uses the treatment beam for imaging, which has less soft-tissue contrast compared to kV imaging. Therefore, radioopaque fiducial markers will be employed for soft tissue target localization, e.g., in prostate radiotherapy. In addition to the advantage of real-time target localization, EPID-based image guidance deserves more clinical attention as it will not cause additional radiation exposure to the patient. Although most modern clinical accelerators are equipped with EPID hardware and the latest models also allow for continuous EPID imaging during advanced beam delivery (e.g., IMRT and VMAT), to the best of our knowledge, real-time EPID-based target localization is still not currently commercially available.

A simple method was proposed for real-time prostate target localization using EPID and implanted fiducial markers during IMRT and VMAT beam delivery [25]. This method uses the beam’s eye view (BEV) gold fiducial positions shown on the EPID image for each MLC segment to determine if there is significant prostate motion/deformation during beam delivery. Manual treatment interruption can be implemented if the fiducial positions are different from their originally planned positions by a preset tolerance/action level. This can be accomplished by a comparison of the BEV fiducial positions on the EPID image and those on the pre-generated DRR (digitally reconstructed radiography) for each MLC segment. To implement this method clinically, software research and development (R&D) by commercial vendors will be necessary to allow for automated DRR generation on a treatment planning system and EPID image acquisition on a treatment machine at preset MLC control points for IMRT delivery and at preset gantry angles for VMAT delivery. In a simple clinical implementation, implanted gold fiducials can be contoured on the simulation CT during treatment planning to generate fiducial volumes (FV) and a uniform (e.g., 4 mm)

margin can be added to the FV to generate their corresponding planning fiducial volumes (PFV). During treatment, the BEV PFV contours can be projected on the EPID image for each MLC segment to facilitate the identification of the fiducial markers, which should appear inside the projected PFV contours if the prostate target has not moved/deformed. This is a simple manual procedure in which a therapist can observe in real time the fiducial positions in comparison to the projected PFV contours and make a decision to interrupt the beam delivery if the fiducials move significantly away from their original positions (i.e., outside the projected PFV). The treatment can be resumed after the fiducial displacement can be resolved, through patient re-positioning or couch offset.

A more advanced implementation of this method would be an automated procedure in which the fiducial markers are automatically detected and their positions accurately calculated. The treatment would be automatically interrupted if the fiducial positions deviated significantly from their original positions (e.g., beyond a preset tolerance/action level); or, a couch movement/MLC leaf tracking could be automatically initiated to correct any significant fiducial displacements [26]. Such an automated procedure would require more R&D efforts from the vendors to provide software solutions for reliable fiducial detection and accurate prostate motion/deformation quantification (and, therefore, the determination of couch offsets). Another obvious restriction in using EPID to monitor prostate motion is the limited field of view (FOV) defined by the MLC leaf opening during IMRT and VMAT treatment delivery. For some particular MLC segments (fields) in the MLC leaf sequence, there might be no fiducial markers present on the EPID image. Therefore, it is necessary to study the time and frequency of observing any fiducial markers within the MLC leaf opening, which can be quantified definitively using the DRRs overlaid with the corresponding MLC leaf pattern based on the patient treatment plan. Even if both hardware and software tools became available clinically, it would still be necessary to know how effectively this method could provide real-time monitoring of prostate motion and displacement correction during modulated beam delivery for different delivery techniques (e.g., IMRT and VMAT).

In this work, we performed a retrospective study on the time and frequency to observe fiducial markers in MLC-modulated fields for intra-fractional prostate motion monitoring and correction based on previously treated prostate IMRT and VMAT plans. A realistic pelvic phantom was used to test the visibility of fiducial markers in modulated fields using EPID and EPID images of the phantom with implanted fiducials were compared with DRRs from the corresponding treatment plans for the phantom. The percentage beam-on time and the time interval for the number of fiducial markers visible within the MLC leaf opening on the DRRs of individual MLC segments/control points were analyzed based on the actual MLC leaf sequences of previously treated IMRT and VMAT patients. An abstract of this work was presented at the 2012 American Association of Physicists in Medicine (AAPM) annual meeting in Miami, Florida [25], and this paper presents the detailed result and data analyses.

2. Materials and methods

2.1 Patient selection

All of the subjects in this study were prostate cancer patients who underwent IMRT or VMAT (RapidArc, Varian Medical Systems, Palo Alto, CA) treatment in the Radiation Oncology Department of Fox Chase Cancer Center from September 2011 to March 2012. A total of 37 cases were selected and divided into three groups: prostate cancer with lymph node metastasis undergoing IMRT (n=14); prostate cancer without lymph node metastasis undergoing IMRT (n=17); prostate cancer patients undergoing VMAT (n=6). The prostate contains soft tissue and lacks traceable structures on EPID images. In order to trace the prostate target accurately, fiducial markers (0.8mm diameter × 3mm long gold seeds, Best Medical International, Springfield, VA) were implanted inside the prostate gland. With fiducial markers as a reference, the prostate target could be localized by tracking the fiducial markers using x-ray imaging. Typically, 3 fiducial markers were implanted for each patient. Occasionally, however, an additional seed was implanted if only two seeds were ideally placed or identifiable on the ultrasound images during the implantation procedure. In the current study, 3–4 gold fiducials were identified in the prostate gland on the simulation CT images of the patients investigated.

2.2 Treatment plan design

The treatment planning system used for this study was Varian Eclipse (V10.0 and V13.6) and the accelerator was Clinac iX (Varian Medical Systems, Palo Alto, CA). All treatment plans were generated with 6 and 10 MV photon beams and optimized to meet our clinical acceptance criteria [1]. The prescription target dose was 76Gy to the prostate and proximal seminal vesicles (Target 1) and 56Gy to the distal seminal vesicles and lymph nodes (Target 2). The rectal dose was limited to V65Gy < 17% and V40Gy < 35%, the bladder dose was limited to V65Gy < 25% and V40Gy < 50%, and the dose to the femoral heads was limited to V50Gy < 10%. For patients treated with static MLC (step-and-shoot) IMRT, 8 or 9 coplanar gantry angles were used with a dose rate of 500 MU/minute while for patients treated with RapidArc, the treatment plans consisted of two arcs: a full arc from 179.9° to 180.1° and a half arc from 225° to 135°. Each arc had 178 control points in the MLC leaf sequence.

2.3. Measurement of fiducial markers using EPID

To test the visibility of implanted fiducial markers (gold seeds) using EPID for prostate IMRT and VMAT, a realistic pelvic phantom (RSD Transparent PIXY Phantom 103–8PL, Radiology Support Devices Inc., Long Beach, CA) was used with three gold seeds placed inside the cavity. The phantom was CT imaged, properly contoured for the treatment target and critical structures (e.g., femoral heads, rectum and bladder) and planned for a standard IMRT treatment using the optimization parameters and acceptance criteria as described in section 2.2. EPID images were taken on a Varian iX accelerator using 6 MV photon beams. The aS1000 EPID detector system has a 40 × 30 cm^2 active imaging area with 1024 × 768 pixel matrix and 30 fps (frames per second) imaging rate. A large square photon field was used for EPID imaging instead of the actual MLC-collimated field. The actual MLC field

shape was later transferred to the EPID image to help confirm whether each fiducial marker was inside or outside the MLC-defined field.

In theory, the number of implanted fiducial markers, which can be observed inside an MLC field, can be predicted by the DRR superimposed with the MLC leaf pattern based on the treatment plan (see section 2.4. below). However, due to organ motion and deformation, the actual number of fiducial markers that can be observed inside the MLC leaf opening may be more or less on the EPID image, assuming the fiducial visibility not being affected by the image quality and/or bony structures. The difference between the locations of the same fiducial marker on the fused DRR and EPID image can be used to determine the movement of the prostate target (assuming no organ deformation). For practical application, a small margin (e.g., 4 mm) can be added to the fiducials to create PFVs during treatment planning and when a fiducial marker on the corresponding EPID image is outside the projected PFV, the treatment can be interrupted and a couch movement can be made to compensate for target displacement. For a simple BEV correction, the in-plane fiducial displacement Δy on the EPID image can be directly applied to the superior-inferior couch shift, and the cross-plane fiducial displacement Δx on the EPID image can be translated into anterior-posterior couch shift by $\Delta x \cdot \sin(\theta)$ and left-right couch shift by $\Delta x \cdot \cos(\theta)$, where θ is the linac gantry angle.

2.4. Evaluation of prostate location with EPID and fiducial markers

Because of the beam modulation in IMRT and VMAT dose delivery, generally, the MLC leaf opening at a typical control point will not cover the beam's eye view (BEV) cross-section of the prostate target. For some particular control points in the MLC leaf sequence, there might be no fiducial markers present on the EPID image. Therefore, it is necessary to study the time and frequency of observing any fiducial markers within the MLC-collimated field, which can be examined definitively using the DRRs overlaid with the MLC leaf pattern of individual MLC segments/control points based on the patient treatment plan. This approach would be more reliable than identifying fiducial markers directly on EPID images taken during patient treatment since the latter could be affected by the EPID image quality, patient anatomy (bony structure) interference and potential prostate motion/deformation.

For IMRT patient plans, DRRs for all MLC segments of the 8 or 9 gantry angles were generated using Eclipse, which were the BEV images containing anatomical structures and fiducial markers. The step-and-shoot delivery technique was used in our clinic with a constant dose rate of 500 MU/minute. The MLC leaf patterns based on the MLC leaf sequences were overlaid on the corresponding DRRs to identify all fiducial markers that were within the MLC leaf opening, which could be used for real-time prostate localization during treatment. The percentage beam-on time for "the number of visible fiducial markers" was calculated using the ratio of the fractional MUs summed up over all MLC segments with the number of fiducial markers visible within the MLC leaf opening to the total MUs for the IMRT treatment. Note that this MU ratio is slightly different from the ratio of the number of MLC segments with visible fiducial markers to the total number of MLC segments for the IMRT treatment because the fractional MUs for individual MLC segments were variable. For VMAT patient plans, the MLC leaf patterns were overlaid on DRR

images of 178 gantry angles/control points of each arc. The fractional MUs were summed up for all control points with the number of fiducial markers visible within the MLC leaf opening and then divided by the total MUs for the VMAT treatment to obtain the percentage beam-on time for "the number of visible fiducial markers". The time interval to observe the number of fiducial markers was calculated by dividing the total beam-on time for the IMRT/VMAT treatment with the total number of MLC segments/control points with the number of visible fiducial markers. For IMRT, the beam-on time included both the MLC leaf movement (step) and radiation (shoot) time while for VMAT, the beam-on time included only the rotation time for the two arcs when the beam was on. The "potential dosimetric uncertainty" associated with the reduced fiducial visibility due to modulated beam delivery is the total dose for a number of consecutive MLC segments with no visible fiducials, during the time interval between two EPID images with visible fiducial markers. This is clearly a worst-case scenario that assumes the entire dose has missed the target during this period of time, which is usually untrue. However, this quantity will be useful in evaluating the method to see whether it is capable to prevent the worst of the possible foreseeable circumstances.

2.5. Statistical analysis

Data were expressed as $\bar{x}\pm s$, where $\bar{x}$ represents the mean value of the investigated quantity of interest and s is the standard deviation of the mean.

3. Results

In order to monitor the location of the treatment target in real time, it is necessary to be able to identify at least one fiducial marker within the MLC defined field on the EPID image. Figure 1 shows typical MLC fields overlaying on the DRRs at different control points of an IMRT leaf sequence. In figure 1(a), two gold fiducials are visible in the MLC opening while in (b), no gold fiducials are available for target localization monitoring.

EPID images have poor soft-tissue contrast but their quality is sufficient for identifying bony structures and implanted gold fiducials. Figure 2 shows DRR and EPID images of a realistic pelvic phantom implanted with 3 gold fiducial markers. It is clear that two fiducial markers are visible for an MLC segment (Fig. 2a and 2b) and three fiducial markers can be observed for another MLC segment (Fig. 2c and 2d). Note that the EPID images were taken with the MLC leaves completely open to show similar fields of view in comparison with the DRRs.

Seventeen IMRT patients included in this study were treated for prostate only (without lymph node involvement). Figure 3 shows the percentage beam-on time when one, two, three or four fiducial markers were visible within the MLC opening during modulated beam delivery for each of the 17 prostate-only patients. Note that patients 13–17 only contained 3 implanted gold seeds in the prostate gland. The mean percentage beam-on time when at least one, two, three or four fiducial markers were visible within the MLC leaf opening during IMRT beam delivery for all gantry angles, was 52±2% (37%−68%), 40±2% (15%−59%), 26±3% (2%−49%) and 19±4% (5%−42%), respectively. For these patients, each IMRT treatment fraction was delivered in 110 ± 20 MLC segments and 10.1 ± 4.1 MU/segment (total MU: 660 – 1560 at a dose rate of 500 MU/minute). The mean time interval to observe at least one fiducial marker was 5.9±0.5 seconds (3.2 – 10.4 seconds), calculated based on

the total beam-on time for the IMRT treatment divided by the number of MLC segments/control points with at least one visible fiducial marker. The potential dosimetric uncertainty for this time interval was estimated to be 3.7 ± 1.5% of the daily dose of 2Gy.

Fourteen patients were treated with IMRT for prostate, seminal vesicles and lymph nodes. Figure 4 shows the percentage beam-on time when one, two, three or four fiducial markers were visible within the MLC opening during modulated beam delivery for 14 IMRT patients treated for both the prostate and lymph nodes. Note that patients 10–14 only had 3 implanted gold seeds. The mean percentage beam-on time when at least one, two, three or four fiducial markers were visible within the MLC opening during IMRT beam delivery for all gantry angles was 42±2% (25%−51%), 30±2% (12%−42%), 15±2% (3%−24%) and 11±1% (4%−15%), respectively. The percentage beam-on time with visible fiducial markers for these patients was generally shorter than that for patients treated for prostate only since some MLC segments were designed specifically to cover the seminal vesicles and lymph nodes where no gold fiducials were implanted. Some large MLC fields had to be split into two on Varian linacs due to deliverability. Therefore, the number of MLC segments and the total MUs increased for these treatments but the MU for each MLC segment deceased slightly (135 ± 25 MLC segments, 920 – 1640 total MU, 9.5 ± 4.3 MU/segment). The mean time interval to observe at least one fiducial marker increased to 8.4 ± 0.7 seconds (5.4 – 12.4 seconds) for these patients and the potential dosimetric uncertainty for this time interval was estimated to be 7.0 ± 2.3% of the daily dose of 2 Gy.

For 6 patients treated using the RapidArc technique, two arcs were used to achieve superior target coverage and critical structure sparing. Figure 5(a) shows the percentage beam-on time during the two-arc modulated beam delivery when one, two and three fiducial markers were visible within the MLC opening for 3 VMAT patients treated for prostate only and figure 5(b) shows the results for 3 VMAT patients treated for both the prostate and lymph nodes. The mean percentage beam-on time when at least one fiducial marker was visible within the MLC opening for the two-arc modulated beam delivery was 88±4% (80% – 94%) for prostate alone and 85±3% (79% – 90%) for prostate plus lymph nodes, respectively. The mean percentage beam-on time when at least two fiducial markers appeared within the MLC opening during the two-arc delivery was 73±8% (58% – 86%) for prostate alone and 59±6% (51% – 72%) for prostate plus lymph nodes, respectively. The mean percentage beam-on time when three fiducial markers were visible within the MLC opening during the two-arc delivery was 59±8% (43% – 70%) for prostate alone and 45±5% (39% – 55%) for prostate plus lymph nodes, respectively. There was a small difference between the full arcs and half arcs; the mean percentage beam-on time with at least one gold fiducial seen within the MLC opening was 81±5% (58% – 91%) for the full arc delivery and 74±6% (53% – 94%) for the half arc delivery, respectively. The mean time interval to observe at least one fiducial marker was 1.6±0.1 seconds (1.4 – 1.7 seconds) and the dosimetric impact of such a small time interval was clinically insignificant (< 1.5% of the daily dose if the target is misaligned during the entire time).

4. Discussion

Advanced conformal radiotherapy treatment techniques such as IMRT and VMAT have garnered popularity in clinical practice. Accordingly, rapid patient setup, accurate target localization, patient dose validation, and real-time organ motion monitoring and correction during treatment have become significantly relevant. EPID was found to be useful in all aspects of image guided advanced radiotherapy treatments [17–24]. The EPID image quality, fiducial marker visibility and recognition/selectivity, and methods/software for marker position reconstruction and prostate motion/rotation determination have been studied extensively, primarily for inter-fractional prostate motion/deformation correction [23,24]. Several studies also reported on-line fiducial marker imaging using continuous EPID and off-line 3D reconstruction of fiducial trajectories to investigate intrafractional motion [27–31]. Kotte et al [27] investigated prostate intrafractional motion for 427 patients by analyzing the positions of implanted fiducial markers on EPID images taken at the first MLC segment of each IMRT gantry angle (5 angles per treatment plan); an in-house program was used to perform the off-line analysis and no online corrections were made. Azcona et al [28] reported results of continuous EPID imaging of prostate motion and offline 3D reconstruction of fiducial trajectories during VMAT treatments for 10 patients. A hybrid kV/MV strategy was also proposed for target localization but no clinical study was performed [29]. Ma et al [30] used on-line EPID images from a single patient treated with IMRT fields for intrafractional motion correction. Since fixed gantry IMRT is not continuous irradiation, the fiducials could move while not being imaged and 3D trajectories could not be reconstructed [29,30]. Brown et al studied the influence of obesity on prostate intra-fractional motion using real-time EPID/fiducials [31]. Xu et al proposed a simple EPID/fiducial-based method for real-time prostate localization during IMRT/VMAT beam delivery [25], which employed EPID imaging to determine the location of the implanted fiducials and to correct prostate motion/deformation based on the BEV fiducial displacement directly. In this work, we performed a retrospective study to investigate the time and frequency for real-time prostate localization using this method during IMRT and VMAT beam delivery.

Currently, the quality of kV grade x-ray imaging is superior to that of MV grade x-ray imaging, but kV grade x-ray imaging requires an independent x-ray source, which increases the complexity and cost of a therapy machine. Onboard kV x-ray imaging, CT-on-rails and CBCT have been used to improve the treatment setup accuracy and efficiency and for inter-fractional motion correction [4–7,32–34]. For those RT machines already equipped with a kV x-ray imaging system, which is used by OBI, KIM and IMR, the imaging beam direction is often perpendicular to the treatment beam direction and if this is the case, only the in-plane target motion can be detected in real time, not the cross-plane organ motion. In addition, the radiation dose generated by kV x-ray imaging increases the risk of second cancers [16]. In comparison, EPID is ideal for real-time target localization because it uses treatment beams to monitor target movement without adding extra radiation doses to the patient, and it can provide both in-plane and cross-plane organ motion information at the same time (i.e., the BEV fiducial displacement). However, EPID images generated by MV photon beams exhibit poor soft-tissue contrast. Thus, this method is only suitable for patients with implanted radio-opaque fiducial markers in or around the target region or for

patients whose target region is close to visible bony structures. Furthermore, the frequent use of EPID to record each MLC segment during IMRT/VMAT beam delivery can result in significant shortening of the life span of the image panel, and, therefore, real-time EPID-based target localization is more suited for hypo-fractionated treatments especially SBRT that delivers much higher prescription target doses with much smaller treatment margins compared to conventional radiotherapy treatments [11]. Further hardware and software developments are warranted to improve the EPID image quality and durability.

With our simple method, EPID is used in combination with the implanted fiducial markers for real-time target localization. The locations of implanted fiducial markers on the EPID images are compared with their positions on the pre-generated DRRs for each MLC segment. If there are significant position changes, the relative displacement of the treatment target can be seen and the treatment can be interrupted, if necessary, based on a preset threshold (i.e., margins can be added to the fiducials to create PFVs for easy visualization and decision making). Since this relative displacement is directly shown in the beam's eye view, a clinical decision can be made by the therapist if the fiducial markers are clearly moving out of the predetermined PFV contours (see Fig. 2). Couch shifts can be made based on the fiducial displacement shown on the EPID image (see method section 2.3). The action levels/tolerances can be pre-determined in treatment planning and no further computation is needed during treatment, similar to the strategy of the Calypso system [8,12,14], where the therapist will interrupt the treatment based on the preset tolerance and make the couch shifts accordingly. This can be performed manually, which will be easy to implement, or automatically with further commercial software implementation. Various methods and software have been investigated to determine fiducial positions and trajectories using sequential (cine) EPID images, which, until now, have been used in offline studies on the trends of prostate motion and deformation/rotation [27–31]. Systematic studies are warranted for automated target localization using EPID/fiducials to ensure the reliability of fiducial recognition/position calculation and the accuracy of motion/deformation correction based on couch shifts/MLC movement [26]. It should be noted that the accuracy of these methods could be compromised by fiducial movements due to real-time organ motion/deformation because the EPID images were taken sequentially.

During radiotherapy treatment, both the position and shape of the prostate can vary due to the gradual filling of the bladder and the rectum, rapid rectal volume change due to gas passage, or patient movement. If one assumes that the prostate only moves without changing its shape, then only one fiducial marker inside the MLC leaf opening is required to monitor the displacement of the target and to make a translational correction. If one further assumes that the prostate rotates but is still rigid, then at least two fiducial markers are required to calculate the translational and rotational change. It is also possible that the prostate deforms due to significant bladder and rectal volume variation, which will change the relative positions of the fiducial markers [14,35]. In this case, at least three fiducial markers are required to determine the deformation of the target volume, and estimate the relative displacement of the treatment isocenter and make any translational and/or rotational motion corrections. Therefore, in order to use EPID and fiducial markers for real-time target localization, a minimum of one fiducial marker must be visible inside the MLC leaf opening to make a translational change of the isocenter. In order to correct translational, rotational

and deformational changes of the prostate target, more fiducial markers must be visible on the EPID image.

Based on the results of our study, for the 17 patients undergoing IMRT for prostate only, at least one fiducial marker was visible within the MLC opening for 52 ± 2% beam-on time (roughly seeing at least one fiducial marker in every other MLC segment, see Figure 3). The mean time interval to observe at least one fiducial marker was 5.9±0.5 seconds (3.2 – 10.4 seconds and the potential dosimetric uncertainty for this time interval was estimated to be 3.7 ± 1.5% of the daily dose, which was about the fractional dose of one MLC segment. For the 14 patients undergoing IMRT for both prostate and lymph nodes, at least one fiducial marker was visible on the EPID image for 42±2% beam-on time (roughly seeing at least one fiducial marker in two-out-of-five MLC segments, see Figure 4). This reduced visibility was due to the large radiation fields needed to cover both target 1 and target 2, which sometimes were divided into two MLC segments on a Varian accelerator (modulated MLC field size was limited to 14.5cm). The mean time interval to observe at least one fiducial marker increased to 8.4 ± 0.7 seconds (5.4 – 12.4 seconds) for these patients and the potential dosimetric uncertainty for this time interval was estimated to be 7.0 ± 2.3% of the daily dose, which was about the dose for two consecutive MLC segments. For the 6 patients receiving VMAT treatment, at least one fiducial marker was visible within the MLC opening during more than 70% of the beam-on time (more than 2 out of 3 control points, see Figure 5), which is more favorable for EPID-based target localization than IMRT treatment. Both full arc and half arc MLC leaf sequences had 178 control points and the fractional MU for each control point/interval was 0.56±0.01% of the total MUs for the arc. The total beam-on time for the two arcs was under 4 minutes. The mean time interval to observe at least one fiducial marker was 1.6±0.1 seconds (1.4 – 1.7 seconds) and the dosimetric impact of such a small time interval was clinically insignificant (< 1.5% of the daily dose, which is about the dose of 2 consecutive MLC control points). It is also observed that those MLC segments that did not show any fiducial markers were often small and delivered less monitor units (MU) and/or aimed at the distal seminal vesicles and lymph nodes (Target 2 prescription dose: 56Gy), which were generally given larger margins and lower localization priority compared to the prostate and proximal seminal vesicles (Target 1 prescription dose: 76Gy).

For more accurate target localization, and in cases where a fiducial marker moved away from its original location and outside the MLC leaf opening, two or more visible fiducial markers on EPID images are desirable. For the 17 IMRT patients treated for prostate only, three fiducial markers were visible within the MLC opening in 36% (11%−67%) of the MLC segments. For the 14 IMRT patients treated for both prostate and lymph nodes, three fiducial markers were visible in 22% (7%−39%) of the MLC segments. Detailed data analyses showed that three or more fiducial markers could be observed after every 3 or 5 consecutive MLC segments for these treatment plans. The mean time interval to observe 3 or more fiducial markers was 8.5 ± 0.7 seconds and the potential dosimetric uncertainty was estimated to be 5.3 ± 2.2% of the daily dose for IMRT of prostate alone. For IMRT treating both the prostate and lymph nodes, the mean time interval was 16.0 ± 1.3 seconds and the potential dosimetric uncertainty was 13.9 ± 4.4% of the daily dose, which is still clinically acceptable considering that there are 38 fractions in a conventional IMRT treatment course. For SBRT treatment with 5 fractions, a 13.9% fractional dose variation would represent a

less than 3% change in the total dose. In this work, two arcs were used for the VMAT plans, which delivered a full arc and a half arc within 4 minutes. Two or more fiducial markers were visible inside the MLC aperture for more than 50% of the MLC control points. This means that these gold fiducials could be seen repeatedly every 2 to 3 seconds. The potential fractional dosimetric uncertainty would be less than 3% even if no gold fiducials were visible for 4 control points consecutively during a VMAT treatment. This indicates that EPID/fiducial-based target localization is more effective for VMAT beam delivery.

It should be mentioned that this work utilized MLC leaf sequences and treatment plan DRRs to quantify the number of visible fiducial markers for target localization instead of counting the actual number of fiducial markers on realistic EPID images, which would yield the "actual" visibility of fiducial markers on EPID during modulated beam delivery for these patients. For a retrospective study, however, the latter was not possible since EPID images were not taken for every MLC segment during the treatment delivery for these patients due to the limitations of our clinical accelerators. On the other hand, our current approach could provide reliable and definitive data analyses of the "theoretical" visibility of fiducial markers (i.e., the best case scenario), without being affected by the EPID imaging quality, patient anatomy interference or organ motion/deformation. It is useful to know both the theoretical and actual fiducial visibility. In this work, we demonstrated the visibility of specific gold fiducial markers on EPID images on our Varian Clinac iX accelerator with 6 MV photon beams. The visibility is expected to be different for other clinical accelerators, EPID models, fiducial types and beam energies. The analyses of time and frequency to monitor gold fiducials in modulated beam delivery were based on 37 previous IMRT/VMAT prostate patients with over 6000 MLC segments/control points. The findings and conclusions of this study were useful and representative of our treatment equipment/technique, which may not be generalizable because of the differences in treatment planning systems, planning strategies/dose constraints, EPID/MLC specifications and delivery techniques (e.g., step-and-shoot vs sliding window). The clinical implementation of EPID/fiducial-based target localization will require both software and hardware changes to the treatment planning system and clinical accelerator in order to compare fiducial positions on TPS-generated DRRs (or projected PFV contours) and those on EPID images. Manual treatment interruption and couch shifts can be performed by the therapist on the treatment machine based on preset action levels/tolerances like other on-line localization systems (Calypso, Vision RT, KIM, IMR, etc). Automated target localization and prostate motion/deformation correction based on EPID/fiducials will require more systematic studies on EPID image quality and commercial hardware/software development so that fiducial monitoring and MLC/couch-based correction can be performed automatically at preset MLC segments for IMRT or preset gantry angles for VMAT. Many small details may affect the "actual" fiducial visibility, e.g., bony anatomy interference, MLC-edge effect and partial fiducial visibility [36]. In some rare cases and for a small number of patients, large and/or sudden prostate excursions may occur frequently [8,14,36], which could impact the patient dose distribution much greater than those dosimetric uncertainties estimated in this work. Nonetheless, we hope that the results of this work will provide sufficient evidence for the TPS/linac vendors to research and develop this functionality and make it clinically available for advanced RT treatments.

5. Conclusion

This work investigated the time and frequency to observe implanted radio-opaque fiducial markers in modulated beam delivery for prostate IMRT/VMAT. This was done by analyzing the percentage beam-on time with the number of fiducial markers visible within the MLC leaf opening based on MLC leaf sequences of 37 previously treated IMRT/VMAT patients. Our results indicated that on the average, at least one fiducial marker was present within the MLC leaf opening for 42±2% and 52±2% of the beam-on time for IMRT of the prostate with and without lymph nodes, and for 85±4% and 88±4% of the beam-on time for VMAT of the prostate with and without lymph nodes, respectively. The estimated potential dosimetric uncertainty associated with reduced fiducial visibility due to modulated beam delivery was 7.0 ± 2.3% and 3.7 ± 1.5% of the daily dose for IMRT of the prostate with and without lymph nodes, respectively, and less than 2% for VMAT of the prostate with and without lymph nodes. Although two or more fiducial markers were sometimes visible inside the MLC defined apertures, which would allow for more accurate calculation and correction for translational, rotational and deformational geometry variations, the probability (i.e., the percentage beam-on time) of seeing more fiducials, unfortunately, decreased reversely with the number of fiducials needed especially with IMRT beam delivery, thus compromising the overall dosimetric accuracy of EPID/fiducial-based target localization.

Acknowledgements

The study was conducted in the Department of Radiation Oncology of Fox Chase Cancer Center. We would like to thank many of our physicians, physicists, dosimetrists and clinical staff for their excellent technical support and useful discussions.

References

[1]. Ma C-M, Adaptive radiation therapy for prostate cancer, in Adaptive Radiation Therapy, Ed. Allen Li X. (CRC Press, New York, 2011) pp331–50.

[2]. Zelefsky MJ, Kollmeier M, Cox B, et al. Improved clinical outcomes with high-dose image guided radiotherapy compared with non-IGRT for the treatment of clinically localized prostate cancer. Int J Radiat Oncol Biol Phys. 2012; 84: 125–129. [PubMed: 22330997]

[3]. Kupelian P, Meyer JL. Image-guided, adaptive radiotherapy of prostate cancer: toward new standards of radiotherapy practice. Front Radiat Ther Oncol. 2011; 43: 344–368. [PubMed: 21625162]

[4]. Feigenberg SJ, Paskalev K, McNeeley S, et al. Comparing computed tomography localization with daily ultrasound during image-guided radiation therapy for the treatment of prostate cancer: a prospective evaluation. J Appl Clin Med Phys. 2007; 8: 2268. [PubMed: 17712295]

[5]. Barney BM, Lee RJ, Handrahan D, et al. Image-guided radiotherapy (IGRT) for prostate cancer comparing kV imaging of fiducial markers with cone beam computed tomography (CBCT). Int J Radiat Oncol Biol Phys. 2011; 80: 301–305. [PubMed: 20864274]

[6]. Ponsky LE, Fuller DB, Meier RM and Ma C-M (Eds), Robotic Radiosurgery Treating Prostate Cancer and Related Genitourinary Applications (Springer-Verlag, Berlin Heidelberg, 2012) DOI: 10.1007/978-3-642-11495-3, Hardcover ISBN: 978-3-642-11494-6, # of pages: 245.

[7]. Keall PJ, Nguyen DT, O'Brien R, Caillet V, Hewson E, Poulsen PR, Bromley R, Bell L, Eade T, Kneebone A, Martin J, Booth JT (2018) The first clinical implementation of real-time imageguided adaptive radiotherapy using a standard linear accelerator. Radiother Oncol 127(1):6–11. [PubMed: 29428258]

[8]. Tong X, Chen XM, Li JS, et al., Intrafractional prostate motion during external beam radiotherapy monitored by a real-time target localization system, J of Applied clinical Med. Phys (2015) 16: 51–60. [PubMed: 26699554]

[9]. Vargas C, Saito AI, Hsi WC, et al. Cine-magnetic resonance imaging assessment of intrafraction motion for prostate cancer patients supine or prone with and without a rectal balloon. Am J Clin Oncol. 2010; 33:11–16. [PubMed: 19730351]

[10]. Gill S, Thomas J, Fox C, et al. Acute toxicity in prostate cancer patients treated with and without image-guided radiotherapy. Radiat Oncol. 2011; 6:145 (7 pages). [PubMed: 22035354]

[11]. Ma C-M. Physics and Dosimetric Principles of SRS and SBRT. Mathews J Cancer Sci. (2019). 4(2): 22 (16 pages).

[12]. Jackson WC, Dess RT, Litzenberg DW, et al., A multi-institutional phase 2 trial of prostate stereotactic body radiation therapy (SBRT) using continuous real-time evaluation of prostate motion with patient-reported quality of life, Practical Radiation Oncology (2018) 8: 40–47. [PubMed: 29304991]

[13]. Meier RM, Bloch DA, Cotrutz C, et al. Multicenter Trial of Stereotactic Body Radiation Therapy for Low- and Intermediate-Risk Prostate Cancer: Survival and Toxicity Endpoints, Int J Radiat Oncol Biol Phys. 2018 102: 296–303. [PubMed: 30191864]

[14]. Li JS, Jin L, Pollack A, Horwitz EM, Buyyounouski MK, Price RA, Ma C-M. Gains from real-time tracking of prostate motion during external beam radiation therapy. Int J Radiat Oncol Biol Phys. 2009 75:1613–20. [PubMed: 19836164]

[15]. Kaur G, Lehmann J, Greer P. et al. Assessment of the accuracy of truebeam intrafraction motion review (IMR) system for prostate treatment guidance. Australas Phys Eng Sci Med 2019 42: 585–598. [PubMed: 31087231]

[16]. Murphy MJ, Balter J, Balter S, BenComo JA, Das IJ, Jiang SB, Ma CM, Olivera GH, Rodebaugh RF, Ruchala KJ, Shirato H, Yin FF. The management of imaging dose during image-guided radiotherapy: report of the AAPM Task Group 75. Med Phys. 2007 34: 4041–63. [PubMed: 17985650]

[17]. van Elmpt W, McDermott L, Nijsten S, Wendling M, Lambin P, Mijnheer B. A literature review of electronic portal imaging for radiotherapy dosimetry, Radiother Oncol. 2008; 88: 289–309. [PubMed: 18706727]

[18]. Kirby MC, Glendinning AG. Developments in electronic portal imaging systems. Br J Radiol 2006; 79: S50–65. [PubMed: 16980685]

[19]. Cremers F, Frenzel T, Kausch C, Albers D, Schonborn T, Schmidt R. Performance of electronic portal imaging devices (EPIDs) used in radiotherapy: image quality and dose measurements. Med Phys 2004; 31: 85–96.

[20]. Lin M-H, Li JS, Wang L, Koren S, Fan JJ, Fourkal E, and Ma C-M, 4D patient dose reconstruction using online measured EPID cine images for lung SBRT treatment validation, Med. Phys (2012) 39: 5949–58. [PubMed: 23039633]

[21]. Ford EC, Mageras GS, Yorke E, et al. Evaluation of respiratory movement during gated radiotherapy using film and electronic portal imaging. Int J Radiat Oncol Boil Phys, 2002, 52: 522–531.

[22]. Poulsen PR, Carl J, Nielson J, et al. Megavoltage image-based dynamic multileaf collimator tracking of a NiTi stent in porcine lungs on a linear accelerator. Int J Rad Onc Biol Phys 2012; 82:e321–e327.

[23]. Van der Heide UA, Kotte ANTJ, Dehnad H, Hofman P, Lagenijk JJW, van Vulpen M, Analysis of fiducial marker-based position verification in the external beam radiotherapy of patients with prostate cancer. Radiotherapy and Oncology (2007) 82: 38–45. [PubMed: 17141903]

[24]. Serago CF, Buskirk SJ, Igel TC, Gale AA, Serago NE, Earle JD. Comparison of daily megavoltage electronic portal imaging or kilovoltage imaging with marker seeds to ultrasound imaging or skin marks for prostate localization and treatment positioning in patients with prostate cancer. Int J Radiat Oncol Biol Phys. 2006; 65: 1585–92. [PubMed: 16863936]

[25]. Xu Q, Lin MH, Chen XM, Tong X, Fan JJ, Dong Z, Chen L, Ma C-M, Feasibility of Using EPID for Real-Time Target Localization during Treatment. Med Phys. 2012 6;39(6Part8):3684. doi: 10.1118/1.4734975.

[26]. Murphy MJ (Eds), Adaptive Motion Compensation in Radiotherapy (CRC Press, Boca Raton, FL, 2012) ISBN: 978-1-4398-2193-0. pp. 33–76.

[27]. Kotte ANTJ, Hofman P, Lagendijk JJW, Vulpen M, van der Heide UA. Intrafraction motion of the prostate during external-beam radiation therapy: analysis of 427 patients with implanted fiducial markers. Int. J. Radiation Oncology Biol. Phys, 2007 69: 419–425.

[28]. Azcona JD, Xing L, Chen X, et al. Assessing the Dosimetric Impact of Real-Time Prostate Motion During Volumetric Modulated Arc Therapy. Int J Radiat Oncol Biol Phys. 2014; 88: 1167–1174. [PubMed: 24661670]

[29]. Liu W, Wiersma RD, Xing L, et al. Optimized hybrid MV-KV imaging protocol for volumetric prostate arc therapy, Int. J. Radiat. Oncol, Biol., Phys (2010) 78: 595–604. [PubMed: 20472354]

[30]. Ma Y, Lee L, Keshet O, et al. Four-dimensional inverse treatment planning with inclusion of implanted fiducials in IMRT segmented fields. Med Phys. 2009; 36: 2215–2221. [PubMed: 19610310]

[31]. Brown A, Tan A, Cooper S and Fielding A, Obesity does not influence prostate intrafractional motion, J Med Radiat Sci (2018) 65: 31–38. [PubMed: 29359862]

[32]. Ng JA, Booth JT, Poulsen PR, et al. Kilovoltage intrafraction monitoring for prostate intensity modulated arc therapy: first clinical results. Int J Radiat Oncol Biol Phys. 2012; 84: e655–e661. [PubMed: 22975613]

[33]. Nguyen DT, O'Brien R, Kim J-H, et al. The first clinical implementation of a real-time six degree of freedom target tracking system during radiation therapy based on Kilovoltage Intrafraction Monitoring (KIM). Radiother Oncol. 2017; 123: 37–42. [PubMed: 28342648]

[34]. Ma C-M and Paskalev K, In-Room CT Techniques for Image-Guided Radiation Therapy, Med. Dosimetry (2006) 31: 30–39.

[35]. Nichol AM, Brock KK, Lockwood GA, et al. A magnetic resonance imaging study of prostate deformation relative to implanted gold fiducial markers. Int J Radiat Oncol Biol Phys 2007; 67: 48–56. [PubMed: 17084546]

[36]. Azcona JD, Li R, Mok E, Hancock S, Xing L. Automatic prostate tracking and motion assessment in volumetric modulated arc therapy with an electronic portal imaging device. International Journal of Radiation Oncology, Biology, Physics. 2013 7;86(4):762–768. DOI: 10.1016/j.ijrobp.2013.03.007.

(a) (b)

Figure 1.
The MLC leaf pattern of each control point overlaying on the corresponding DRR for an IMRT patient to show the number of fiducial markers visible in the MLC leaf opening: (a) two, and (b) zero.

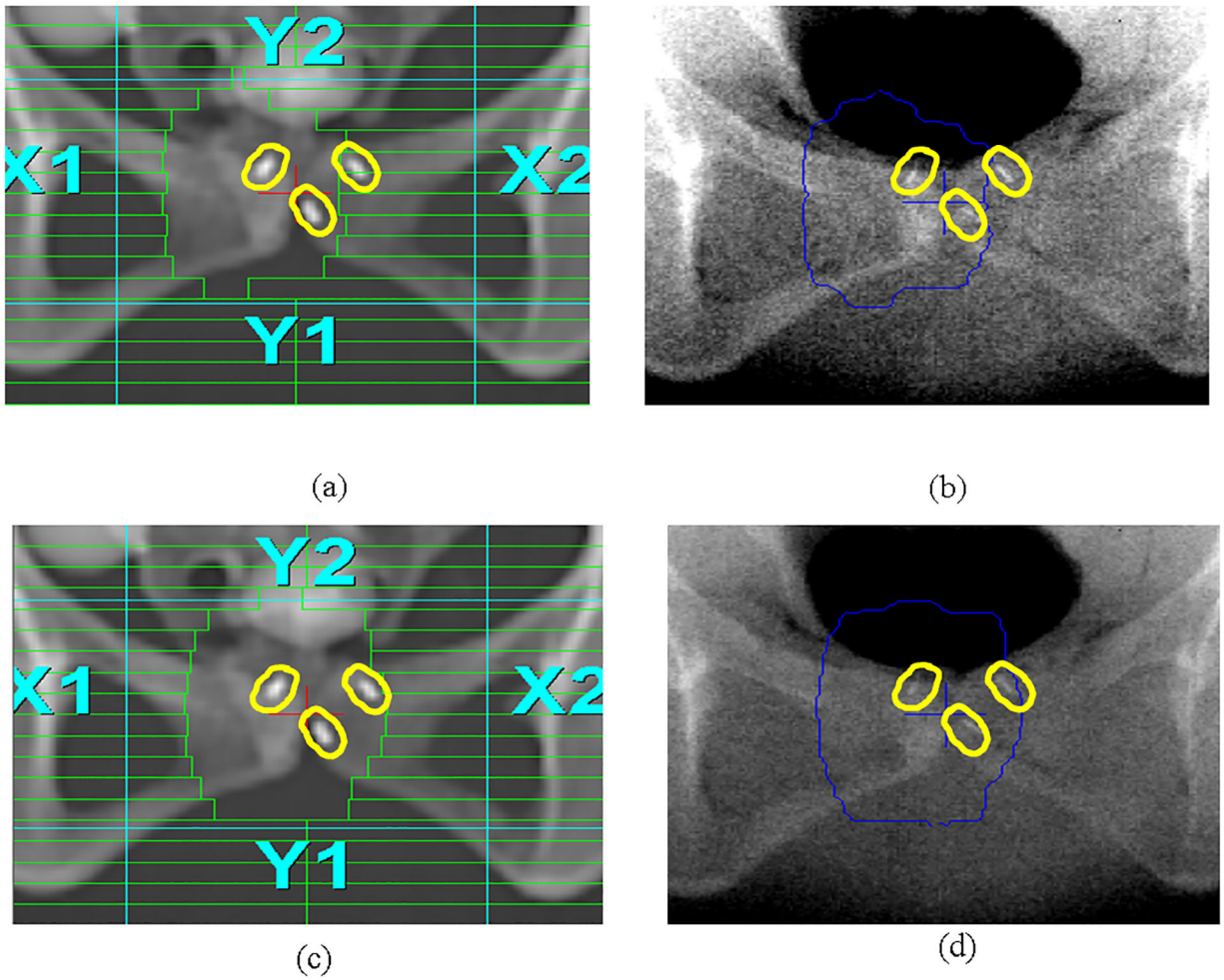

Figure 2.

The MLC leaf pattern of a control point overlaying on the DRR for a pelvic phantom (a) showing 2 visible gold seeds in the MLC opening, and on the EPID image (b). Three gold seeds are visible in another MLC opening on DRR (c) and on EPID (d). A uniform 4mm margin was added to the gold fiducials in treatment planning to form their corresponding PFVs, to facilitate fiducial identification on EPID and to define the tolerance/action level.

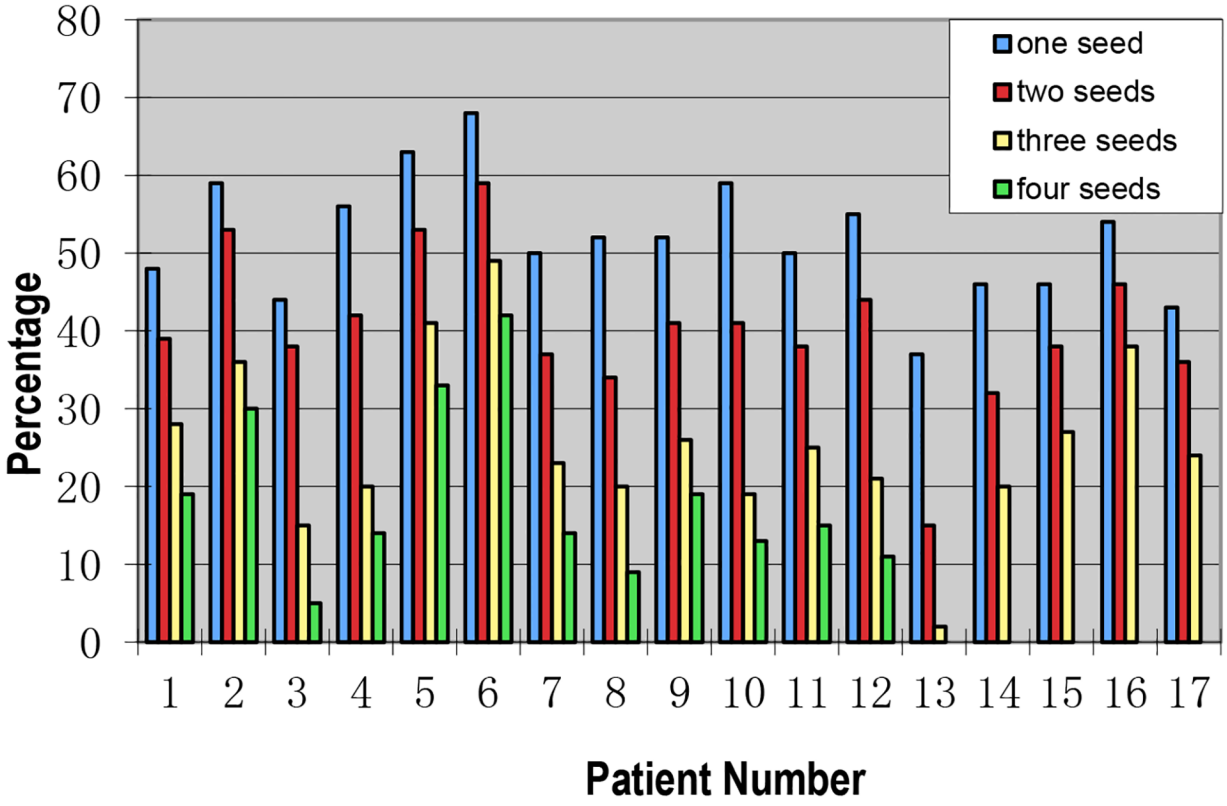

Figure 3.
The percentage beam-on time with one, two, three or four visible gold seeds within the MLC leaf opening during modulated beam delivery for 17 prostate-only IMRT patients.

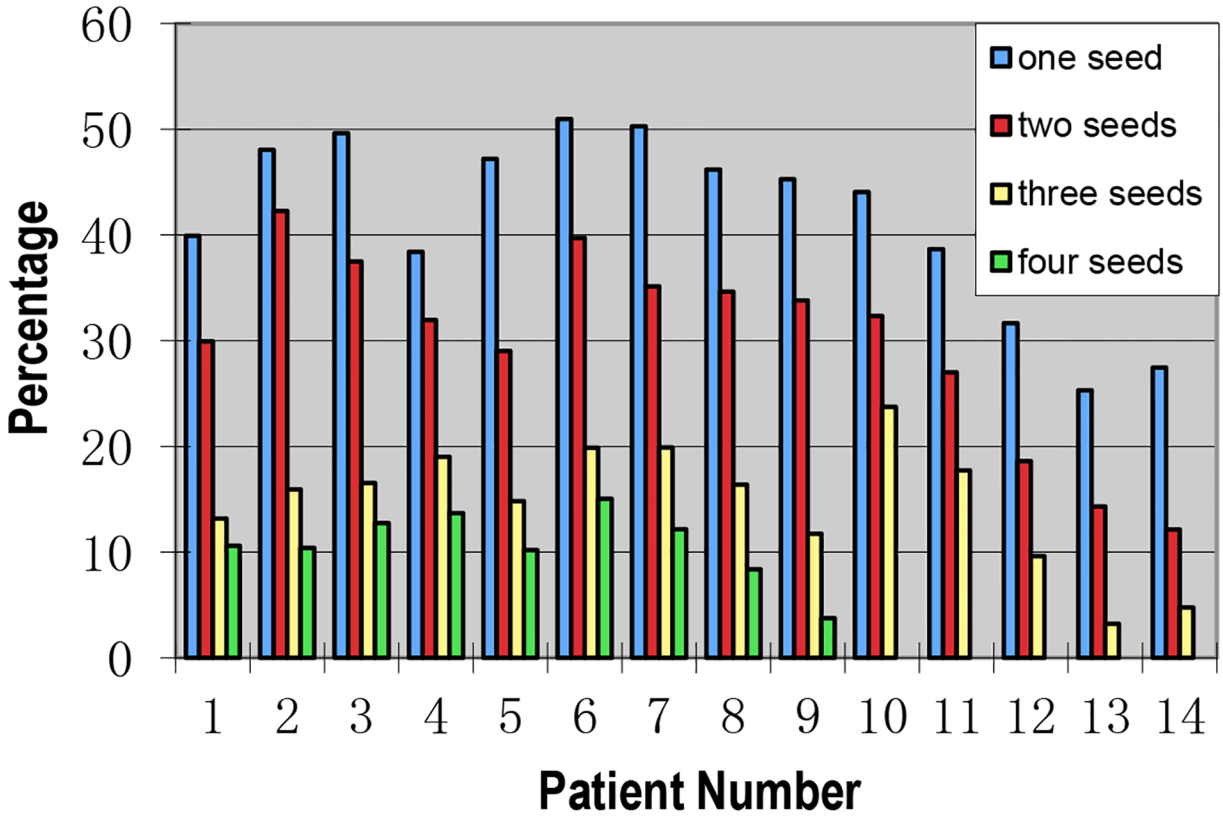

Figure 4.

The percentage beam-on time with one, two, three or four visible gold seeds within the MLC leaf opening during modulated beam delivery for 14 IMRT patients treated for both the prostate and lymph nodes.

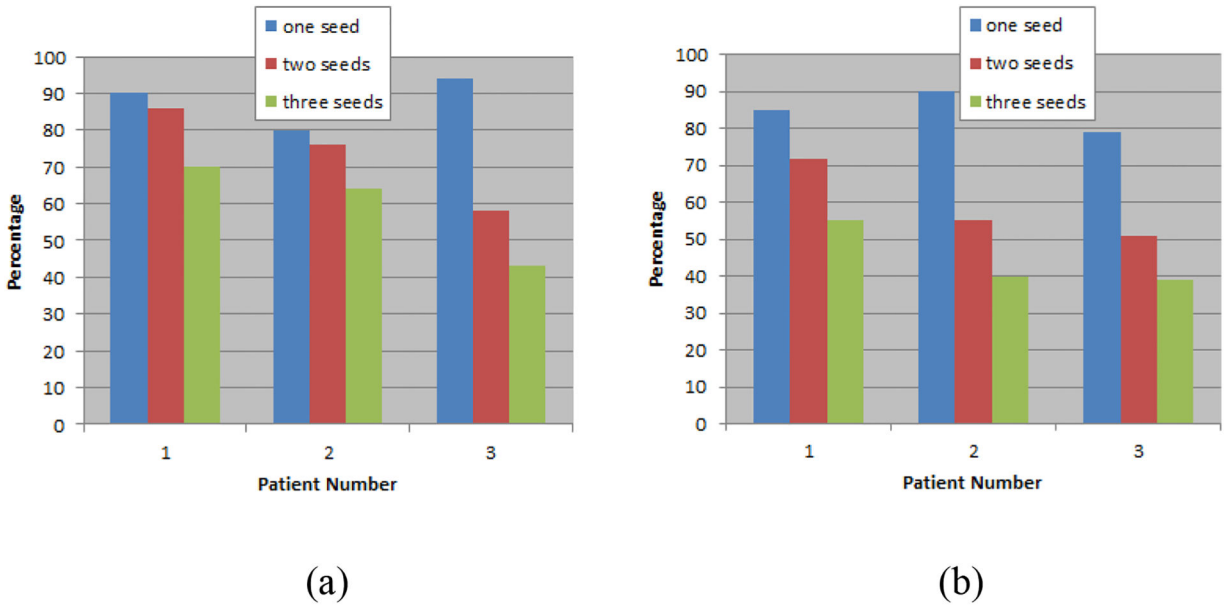

Figure 5.

The percentage beam-on time with one, two and three visible gold seeds within the MLC leaf opening for 3 VMAT patients treated for prostates only (a) and for both prostates and lymph nodes (b).